Oxidative removal of Cu from carbon-saturated iron via Ag phase into B_2O_3 flux

Hideki ONO and Katsuhiro YAMAGUCHI*
Division of Materials and Manufacturing Science, Graduate School of Engineering, Osaka University,
2-1 Yamadaoka, Suita, Osaka 565-0871, Japan

Abstract: The oxidative removal of Cu from carbon-saturated iron via the Ag phase into B_2O_3 flux was attempted at 1523 K. The Cu content was reduced from 4 to below 0.2 mass%, and Cu in the molten iron could be removed into the B_2O_3 flux by the method proposed in this study. Furthermore, the Cu distribution ratio between the B_2O_3 flux and Ag, $L_{Cu(flux\text{-}Ag)}$ (= [mass% Cu]$_{(in\ flux)}$ / [mass% Cu]$_{(in\ Ag)}$) and the dependence of the activity coefficient of Cu_2O in the B_2O_3 flux, $\gamma_{Cu(in\ flux)}$, on the oxygen partial pressure were measured. The greatest value of $L_{Cu(flux\text{-}Ag)}$ was found to be 17 at 0.6 atm of oxygen partial pressure. Using this value, the distribution ratio of Cu between the B_2O_3 flux and carbon-saturated iron, $L_{Cu(flux\text{-}Fe)}$ (= [mass% Cu]$_{(in\ flux)}$ / [mass% Cu]$_{(in\ Fe\text{-}C))}$) is calculated to be 120 at 1523 K. A numerical calculation of mass transfer on the solutes in the Ag phase is performed, and the optimum condition on the removal of Cu by the method proposed in this work is discussed.

Key words: Tramp element, Copper, Iron scrap, Recycle, Oxidation

1. Introduction

In Japan, approximately 30 million tons of waste steel scrap is purchased every year, and approximately 3 million tons thereof is exported[1]. Almost all of the iron ore and coal consumed in Japan are imported and so, waste scrap is a valuable iron source and should be recycled as far as possible. Furthermore, recycling the thermochemically-reduced steel scrap reduces carbon dioxide emissions. However, waste steel scrap contains Cu and Sn, which are deleterious elements in steel-making and cannot be removed by oxidizing-refining in a conventional steelmaking process. Therefore, these elements accumulate in the molten iron, and it becomes a major problem in recycling steel scrap with Cu being the most troublesome element. The amount of available waste steel scrap with low Cu content is declining, and the scrap with higher Cu content is difficult to recycle without diluting the Cu content with pig iron. Therefore, the establishment of an industrial method for removing Cu from iron is on urgent necessity.

Cu attached to steel scrap can be removed by advanced magnetic separation after shredding or Cu dissolution into a solvent such as molten Al[2-4] or aqueous NH_3 solution[5]. However, complete separation of the Cu from the steel is difficult in reality, and the dissolution of some of the Cu into the molten iron is unavoidable.

The liquid phase of the Fe-Cu binary system is miscible over the whole composition range. It has been reported that the liquid separates into Fe-rich and Cu-rich phases by adding C[6,7] and B[8]. However, the Cu content of the Fe-rich phase is approximately 5 mass%, and it is difficult to use this Fe-rich phase as an iron source. On the other hand, using the immiscibility of Ag and Pb in Fe, the reduction of the Cu content of the Fe phase has been achieved by the distribution of Cu between the Fe and Ag (Pb) phases[7]. However, because the distribution ratio of Cu between Ag (Pb) and Fe is insufficient, the quantity of Ag (Pb) necessary for this removal treatment is large and this method is not

economically viable. We have proposed and attempted the oxidative removal of Cu[9] and Sn[10] from Fe-C(satd.) via Ag, and the Cu and Sn contents of the Fe-C(satd.) have been decreased to 0.4 mass% and below 0.001 mass%, respectively. The lower limit of Cu in the Fe-C(satd.) can be decreased by absorbing the Cu oxide into the flux. Therefore, it is important to find the flux which has higher absorption ability of the Cu oxide. Accordingly, in this work, the activity coefficient of Cu_2O in the B_2O_3 flux is measured. In addition, the oxidative removal of Cu from the Fe-C(satd.) via the Ag phase into the B_2O_3 flux is performed at 1523 K.

2. Principle of the oxidative removal of Cu from molten iron via Ag into the B_2O_3 flux

It is impossible to remove Cu in molten iron by the oxidative refining because the molten iron is oxidized in preference to Cu, in principle. Accordingly, in this work, Ag is used as a solvent for Cu because Ag and Fe are immiscible and Cu is oxidized in preference to Ag. A schematic diagram of the oxidative removal of Cu from iron via Ag phase is shown in Fig. 1. The distribution of Cu between Fe-C(satd.) and Ag is expressed as shown in Eq. (1):

$$\underline{\mathrm{Cu}}_{(\text{in Fe-C})} = \underline{\mathrm{Cu}}_{(\text{in Ag})} \tag{1}$$

The oxidation reaction of Cu in the Ag is expressed as shown in Eq. (2):

$$\underline{\mathrm{Cu}}_{(\text{in Ag})} + \frac{1}{2}\mathrm{O}_2(\mathrm{g}) = \frac{1}{2}\mathrm{Cu}_2\mathrm{O}(\mathrm{l}) \tag{2}$$

By combining Eqs (1) and (2), Eq. (3) is obtained, and the oxidative removal of Cu from molten iron is possible without oxidation of the Fe-C(satd.). The lower limit of Cu content of the Fe-C(satd.) is calculated from the equilibrium relation of Eq. (3) and is shown in Eq. (4)

$$\underline{\mathrm{Cu}}_{(\text{in Fe-C})} + \frac{1}{2}\mathrm{O}_2(\mathrm{g}) = \frac{1}{2}\mathrm{Cu}_2\mathrm{O}(\mathrm{l}) \tag{3}$$

$$N_{\mathrm{Cu(in\ Fe\text{-}C)}} = \frac{a_{\mathrm{Cu_2O}}^{1/2}}{\gamma^{\circ}_{\mathrm{Cu(in\ Fe\text{-}C)}} K_{(3)} p_{\mathrm{O_2}}^{1/2}} \tag{4}$$

where $N_{i(\text{in } j)}$, $K_{(3)}$, $\gamma^{\circ}_{i(\text{in } j)}$, $p_{\mathrm{O_2}}$ and a_i are the mole fraction of *i* in *j*, the equilibrium constant of Eq. (3) (= 9.71×10^{-3})[11], the activity coefficient of *i* in *j* at infinite dilution in the pure substance reference, the partial pressure of oxygen and the activity of *i* relative to the pure substance, respectively. By substituting for $\gamma^{\circ}_{\mathrm{Cu(in\ Fe\text{-}C)}}(=50.2)$ [9], $p_{\mathrm{O_2}}(=1\mathrm{atm})$ and $a_{\mathrm{Cu_2O}}(=1)$, $N_{\mathrm{Cu(in\ Fe\text{-}C)}}$ is calculated to be 1.96×10^{-3} (0.26 mass%), and this value is the lower limit of Cu at the conditions of $p_{\mathrm{O_2}}(=1\mathrm{atm})$ and $a_{\mathrm{Cu_2O}}(=1)$. In Eq. (4), the Cu content of the Fe-C(satd.) can be more decreased by decreasing $a_{\mathrm{Cu_2O}}$. Besides, the oxide flux, which is melted at the operating temperature and has a strong affinity for Cu_2O, should be selected for decreasing $a_{\mathrm{Cu_2O}}$, effectively.

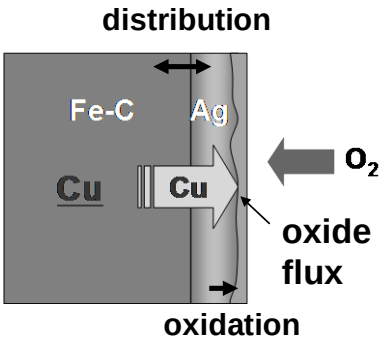

Fig. 1 Schematic representation of the oxidative removal of Cu into oxide flux via Ag phase proposed in this study.

Morinaga *et al.*[12] regarded the basicity of slag as the quantity which was proportional to the reciprocal of the coulomb force between cation and oxide ion and proposed the basicity parameter, *B*, as shown in Eq. (5)

$$B_i' = \left[\frac{z_i \times 2}{(r_i + 1.40)^2} \right]^{-1}$$
$$B_i = \frac{B_i' - B_{SiO_2}'}{B_{CaO}' - B_{SiO_2}'} \quad (5)$$
$$B = \sum_i n_i B_i$$

where z_i, r_i and n_i are electrical charge, ion radius (Å) and mole ratio of cation *i*, respectively. Values of the basicity parameter, *B*, of representative oxides are shown in Table 1. In Table 1, oxides with large *B* are strongly basic. Because Cu_2O is classified as a basic oxide, oxides such as B_2O_3 and SiO_2 which are classified as acidic oxides seem to have a large capacity of Cu oxide. The melting point of B_2O_3 is 753K and is lower than the experimental temperature of this work, 1523K. The activity curve of the B_2O_3-Cu_2O system is calculated at 1523 K, using *FactSage 6.1* and is shown in Fig. 2. The B_2O_3-Cu_2O system has a negative bias, and the B_2O_3 is expected to have a large capacity of Cu oxide. In this work, the activity coefficient of Cu_2O in the B_2O_3 flux, $\gamma_{Cu_2O(\text{in flux})}$, is measured to determine the capacity of Cu oxide. Besides, the oxidative removal of Cu from the Fe-C(satd.) via Ag into the B_2O_3 flux is attempted. The quantity of Ag needed for the oxidation removal is low, in principle, because Ag is used as an intermediary phase for the oxidative removal of Cu. Carbon plays an important role in lowering the melting point of iron and raising the distribution ratio of Cu between the Ag and Fe, $L_{Cu(Ag\text{-}Fe)}$ (= [mass% Cu]$_{(\text{in Ag})}$ / [mass% Cu]$_{(\text{in Fe(-C)})}$).

Table 1 Values of the basicity parameter, *B*, of representative oxides.

Oxide	B
K_2O	3.381
Na_2O	2.349
Cu_2O	2.326
Li_2O	1.719
BaO	1.561
PbO	1.307
SrO	1.269
CaO	1.000
SnO	0.931
FeO	0.723
ZnO	0.723
CuO	0.703
MgO	0.641
Bi_2O_3	0.512
Fe_2O_3	0.282
Ga_2O_3	0.269
Al_2O_3	0.198
ZrO_2	0.190
SnO_2	0.148
TiO_2	0.133
TeO_2	0.078
GeO_2	0.045
B_2O_3	0.026
SiO_2	0.000
P_2O_5	-0.103

3. Experimental

The experimental apparatus consisted of a mullite tube (70 mm outer diameter, 60 mm inner diameter, 1000 mm length) and a vertical $MoSi_2$ electric resistance furnace connected to a proportional integral derivative action controller with a Pt-6%Rh/Pt-30%Rh thermocouple.

3.1 Measurement of the activity coefficient of Cu_2O in the B_2O_3 flux

The experimental conditions are shown in Table 2. Ten grams of reagent grade Ag (purity: 99.9%), 0.20-0.22 g of reagent grade Cu (purity: 99%) and reagent grade B_2O_3 (purity: 99.9%) were charged in an alumina crucible (38 mm outer diameter, 45 mm height, 30 cm^3 capacity). The crucible was inserted into an alumina crucible (52 mm outer diameter, 42 mm inner diameter, 100 mm height), and the sample was melted in the furnace under argon atmosphere at 1523 K. Then, the oxygen and argon mixture (total flow rate: 150 cm^3/min (s.t.p.), p_{O_2} : 0.1–1 atm) was blown onto the Ag-Cu alloy from 20 mm above the surface of sample for over 1–12 h. After the equilibrium was attained, the alumina crucible was withdrawn from the furnace, and the sample was quenched rapidly under argon gas flow. The Cu content of the Ag and the Ag, Cu, Al and B contents of the flux were analyzed by an inductively coupled plasma-atomic emission spectrometry (ICP-AES).

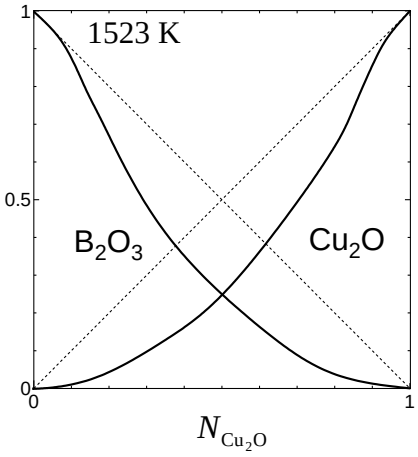

Fig. 2 Activity curve of Cu_2O-B_2O_3 system at 1523 K.

Table 2 Experimental conditions of the measurement of the activity coefficient of Cu_2O in the B_2O_3 flux at 1523 K.

No.	Initial mass of reagent (g)			Time (h)	p_{O_2} (atm)
	Ag	Cu	B_2O_3		
1	10	0.20	0.45	6	0.1
2	10	0.20	0.50	6	0.4
3	10	0.20	0.50	6	0.6
4	10	0.21	0.46	6	0.6
5	10	0.21	0.51	1	1
6	10	0.20	0.46	6	1
7	10	0.22	0.50	12	1
8	10	0.22	0.97	12	1

3.2 Oxidative removal of Cu from carbon-saturated iron via Ag phase into B_2O_3 flux

The alumina crucibles and tubes shown in Figs. 3 (a) (Run 9), (b) (Runs 10–17) were used in the experiments with the experimental conditions shown in Table 3. Runs 9–11 were performed without B_2O_3. The B_2O_3 and B_2O_3-Al_2O_3-Ag_2O fluxes used for the experiments were preliminary made in the following manner, and the compositions of these fluxes were analyzed by ICP-AES:

(1) B_2O_3 flux: the reagent B_2O_3 contained in an alumina crucible (38 mm outer diameter, 45 mm height, 30 cm^3 capacity) was inserted into the furnace at 1523 K under an argon atmosphere for 3 h. The Al_2O_3 content of the flux was 0.4 mass%, and this value is lower than the solubility from the phase diagram of the B_2O_3-Al_2O_3 system (approximately 4 mass%) [13].

(2) B_2O_3-Al_2O_3-Ag_2O flux: the reagent B_2O_3 and sufficient mass of reagent Ag were contained in the alumina crucible (38 mm outer diameter, 45 mm height, 30 cm^3 capacity) and inserted into the furnace at 1523 K under an argon atmosphere, and the B_2O_3 and Ag were pre-melted. An alumina tube (3 mm outer diameter, 2 mm inner diameter) was inserted in the melt, and oxygen gas (150 cm^3/min (s.t.p.)) was blown into the melt for 1.5 h. The B_2O_3- 6~7 mass%Al_2O_3-15 mass%Ag_2O was obtained.

A small path was made at the lowest point of the alumina tube (21 mm outer diameter, 16 mm inner diameter, 50 mm length), and the tube was set in the alumina crucible as shown in Figs. 3 (a) and (b). The reagents Ag and Cu were weighed and placed in- and out-side the alumina tube. A graphite tube was inserted into the alumina tube, and the prepared Fe-4 mass% Cu-C(satd.) alloy was placed in the graphite tube. A graphite lid was placed on the graphite tube and the alumina tube was sealed with an alumina lid and cement. The alumina crucible was placed in an alumina crucible (52 mm outer diameter, 42 mm inner diameter, 100 mm height) and was inserted into the furnace under an argon atmosphere (100 cm^3/min (s.t.p.)) at room temperature. The furnace was heated to 1523 K for 2.5 h. In Run 11, oxygen gas (15 cm^3/min (s.t.p.)) was blown into the Ag from the alumina tube (3 mm outer diameter, 2 mm inner diameter) for 0.5 h. In Runs 12–17, oxygen gas (150 cm^3/min (s.t.p.)) was blown onto the Ag from the alumina tube which was set approximately 40 mm above the metal surface. For Runs 9–13, the samples were pre-melted at 1373 K under an argon atmosphere (100 cm^3/min (s.t.p.)) for 0.5 h to melt the Ag-Cu alloy, and the furnace was heated to 1523 K and was held for 0.5 h to distribute Cu between the Ag and Fe-C(satd.). Thereafter, oxygen gas was blown onto the flux. After the experiments, the alumina crucible was withdrawn from the furnace, and the sample was quenched rapidly under argon. The Cu content of the Ag, the Cu and Ag contents of the Fe-C(satd.) and the Cu, Ag, Al and B contents of the flux were analyzed by ICP-AES. The powder X-ray diffraction spectrum analysis of the oxides which were formed at the path in Run 9 was performed. The Ag both in- and out-side the alumina tube was chemically analyzed separately. In this work, the C content of the Fe-C (satd.) was approximately 4.5 mass%[9].

Table 3 Experimental conditions of oxidative removal of Cu from carbon-saturated iron via Ag phase into B_2O_3 flux at 1523 K.

No.	Flux	Ag (g)	Cu (g)	Fe alloy(g)	[mass% Cu] (in Fe)	Flux (g)	p_{O_2} (atm)	Time (h)	Flow rate (cm^3/min)
9		30	0.61	9.9	3.0			7	15
10	-	65	2.0	7.4	3.0	-	1	0.25	100
11		65	2.0	7.7	3.9			0.5	15
12	B_2O_3-Al_2O_3	60	0.55	8.0	3.9	3.5	1	3	150
13		60	0.17	8.0	3.9	3.6		3	
14	B_2O_3-Al_2O_3-Ag_2O	59	0.55	7.9	3.9	6.0	1	1	150
15		60	1.0	7.9	3.9	3.5		3	
16		59	0.56	7.9	3.9	6.0		1	
17		60	1.0	7.8	3.9	3.7		3.5	

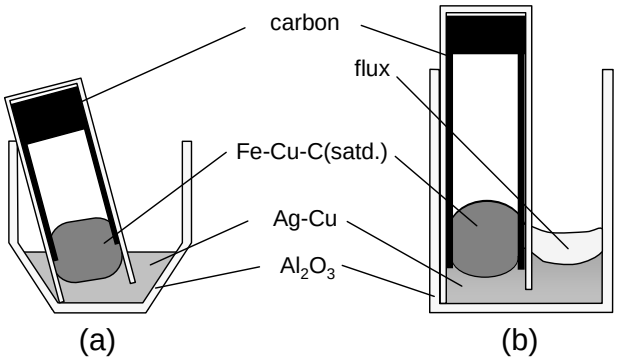

Fig. 3 Schematic cross section of the experimental arrangement of the crucible.

4. Results

4.1 Measurement of the activity coefficient of Cu_2O in the B_2O_3 flux

The experimental results are shown in Table 4. The components of flux are assumed to be B_2O_3, Cu_2O, Al_2O_3 and Ag_2O. The distribution ratio of Cu between the *i* and *j* phases is defined by $L_{Cu(i-j)}$(=[mass% Cu]$_{(in\ i)}$/ [mass% Cu]$_{(in\ j)}$). In our previous work, the Cu content of the Ag was approximately 1.5 mass%, which was measured without oxide flux in an oxygen atmosphere (1 atm) at 1523 K[9]. In contrast with the previous work, the Cu content of the Ag of this work (Runs 1–8) is below 1.5 mass%, which shows that the B_2O_3 flux has an absorption capacity for Cu_2O. The variation of the Cu content of the Ag with time is shown in Fig. 4 for the experiments performed in an oxygen atmosphere (1 atm) and for the same initial mass ratio of B_2O_3 against Cu (approximately 2). As shown in Fig. 4, the Cu content of the Ag already reaches a constant value after 1 h. Therefore, the equilibration time is judged to be less than 1 h, but the other experiments were performed for longer than 6 h to give sufficient time for equilibration. For Runs 1–7, the dependences of the Cu contents of the Ag and flux on p_{O_2} are shown in Fig. 5. From the results in Fig.5, the dependence of $L_{Cu(flux-Ag)}$ on p_{O_2} is shown in Fig. 6. The greatest value of $L_{Cu(flux-Ag)}$ is 17 at a partial oxygen pressure of 0.6 atm under the experimental conditions in this work. The dependence of the Ag content of the flux on p_{O_2} is shown in Fig.

7. The Ag content of the flux rises with an increase in p_{O_2}.

Table 4 Experimental results of the measurement of the activity coefficient of Cu_2O in the B_2O_3 flux.

No.	In Ag (mass%)	In oxide flux (mass%)				L_{Cu} (flux-Ag)	Flux composition (mole fraction)				γ_{Cu_2O}
	Cu	Cu	Ag	Al	B		N_{Cu_2O}	N_{Ag_2O}	$N_{Al_2O_3}$	$N_{B_2O_3}$	
1	0.779	7.1	26.6	8.5	7.22	9.1	0.084	0.184	0.234	0.498	0.676
2	0.543	7.3	35.4	9.9	7.66	13.4	0.076	0.216	0.242	0.467	0.729
3	0.475	8.0	38.1	10.1	7.45	16.8	0.082	0.229	0.242	0.447	0.634
4	0.492	7.6	39.3	9.9	7.53	15.4	0.077	0.236	0.236	0.451	0.719
5	0.499	7.5	39.0	9.3	7.19	15.1	0.079	0.242	0.232	0.447	0.927
6	0.537	8.0	40.5	10.5	4.08	14.8	0.099	0.297	0.306	0.298	0.861
7	0.638	8.3	38.6	10.8	3.63	13.0	0.106	0.292	0.327	0.275	1.128
8	0.352	5.1	41.7	10.8	4.79	14.6	0.062	0.295	0.306	0.338	0.595

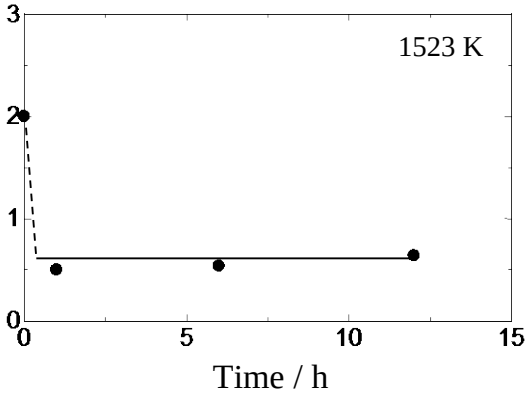

Fig. 4 The variation of the Cu content of the Ag with time at 1523 K.

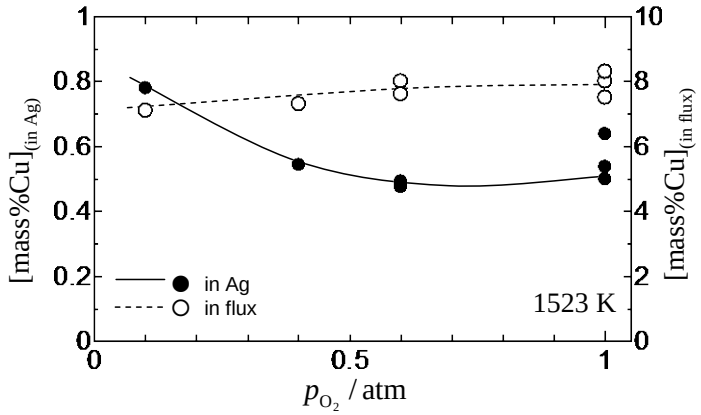

Fig. 5 Dependences of the Cu contents of the Ag and flux on p_{O_2} at 1523 K.

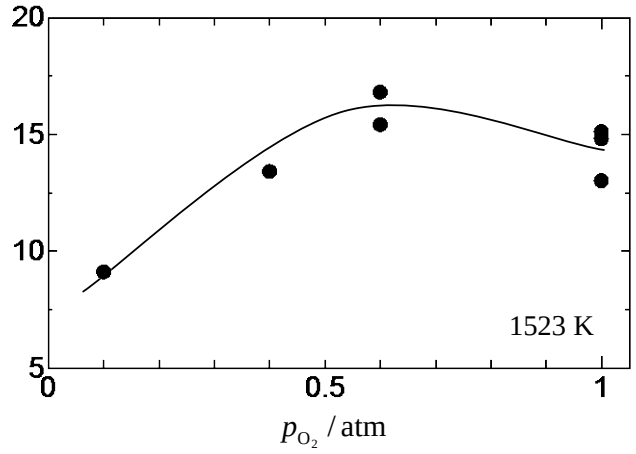

Fig. 6 Dependence of $L_{Cu(flux-Ag)}$ on p_{O_2} at 1523 K.

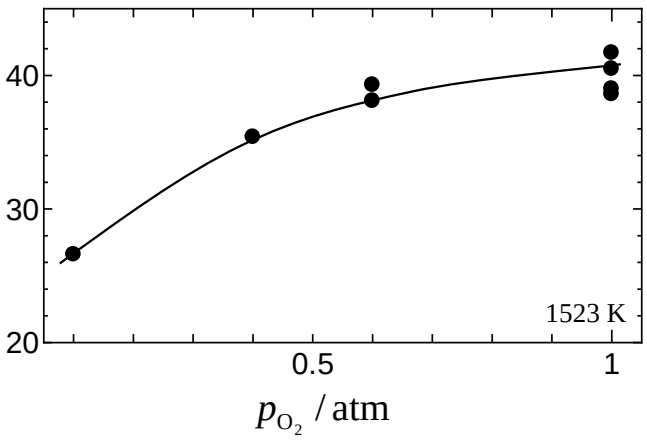

Fig. 7 Dependence of the Ag content of the flux on p_{O_2} at 1523 K.

4.2 Oxidative removal of Cu from carbon-saturated iron via Ag into B_2O_3 flux

The experimental results are shown in Table 5. The Cu content of the Ag and Fe-C(satd.) before oxidation is calculated from the initial mass of Fe, Ag and Cu and $L_{Cu(Ag-Fe)}$ (=7.15)[9] and is also shown in Table 5. In Runs 9 and 11, the Cu contents of the Fe-C(satd.) and Ag are confirmed to be decreased from those before oxidation. In Run 10, the molten iron moves outside of the alumina tube, and iron oxide is formed. In the experiments performed with B_2O_3(-Al_2O_3-Ag_2O) flux (Runs 12–17), the experimental results are classified into three types: (1) Both the Cu and Ag contents of the flux are low and the Cu contents of the Fe-C(satd.) and Ag phases do not decrease (Runs 12 and 13), (2) The Cu is dissolved into the B_2O_3 flux and the Fe is not dissolved (Runs 14 and 15), (3) Both the Cu and Fe are dissolved into the B_2O_3 flux (Runs 16 and 17). For Runs 15-17, the Cu content of the Ag inside the alumina tube cannot be measured because there is an inadequate amount of the Ag phase present. From the result of Run 14, it has been clarified that the Cu content of the Fe-C(satd.) can be decreased to below 0.2 mass% with the B_2O_3-Al_2O_3-Ag_2O flux.

In Run 9, the Cu content of the Ag in- and out-side the alumina tube differs, and the distribution ratio of the Cu between the Ag inside the alumina tube and the Fe phases, $L_{Cu(Ag(inside)\text{-}Fe)}$, corresponds to the equilibrium value. The powder X-ray diffraction pattern of the oxides formed at the path in Run 9 is shown in Fig. 8. $FeAl_2O_4$ is identified, and the Cu transfer in the Ag phase is considered to be blocked at the path by the formed $FeAl_2O_4$.

Table 5 Experimental results of the oxidative removal of Cu from carbon-saturated iron via Ag into B_2O_3 flux.

No.	Before oxidation (calc.) (mass%)		Experimental result (mass%)									$L_{Cu(Ag\text{-}Fe)}$	
	(in Ag)	(in Fe)	(in Ag)		(in Fe)		(in B_2O_3)						
	Cu		Cu (outer)	Cu (innner)	Cu	Ag	Cu	Ag	B	Fe	Al	(outer)	(inner)
9	2.92	0.41	2.75	1.61	0.38	0.08						4.2	7.2
10	3.27	0.46	-	-	-	-			-			-	-
11	3.53	0.49	3.22	3.12	0.47	0.06						6.6	6.9
12	1.40	0.20	1.47	1.37	0.18	0.06	0.068	0.193	30.6	0.51	1.46	8.3	7.0
13	0.79	0.11	0.81	0.78	0.11	0.07	0.044	0.151	32.1	0.49	1.46	7.3	7.1
14	1.48	0.21	1.25	1.36	0.19	0.06	1.73	17.9	20.0	0.19	9.46	6.5	6.6
15	2.13	0.30	1.72	-	0.29	0.09	6.89	25.2	14.4	1.71	10.7	6.0	-
16	1.49	0.21	1.37	-	0.20	0.07	0.98	9.81	21.1	4.61	9.71	7.0	-
17	2.11	0.30	1.71	-	0.41	0.12	2.08	3.77	10.3	27.4	11.6	4.1	-

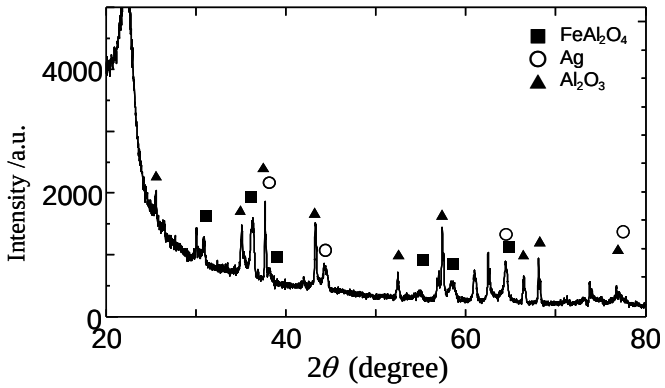

Fig. 8 Powder X-ray diffraction pattern of the oxides formed in Run 9.

5. Discussion

5.1 Activity coefficients of Cu_2O and Ag_2O in the B_2O_3 flux

The activity coefficient of the Cu_2O in the flux, $\gamma_{Cu_2O(in\ flux)}$, is represented by Eq. (7) from the equilibrium of Eq. (6).

$$2Cu(l) + 1/2O_2(g) = Cu_2O(l) \tag{6}$$

$$\gamma_{Cu_2O(in\ flux)} = \frac{\gamma^{\circ}_{Cu(in\ Ag)} N^2_{Cu(in\ Ag)} p^{1/2}_{O_2} K_{(6)}}{N_{Cu_2O(in\ flux)}} \tag{7}$$

The value of the $\gamma_{Cu_2O(in\ flux)}$ is calculated by substituting $K_{(6)}$ (=9.71×10^{-3})[11], $\gamma^{\circ}_{Cu(in\ Ag)}$ (= 3.14) [14] and the

experimental conditions and results into Eq. (7). The dependence of $\gamma_{Cu_2O(\text{in flux})}$ on $N_{B_2O_3(\text{in flux})}$ is shown in Fig. 9. The $\gamma_{Cu_2O(\text{in flux})}$ value decreases with an increase in $N_{B_2O_3(\text{in flux})}$. From the results, the B_2O_3 flux has an affinity for Cu_2O, and it is possible to remove the Cu into the B_2O_3 flux.

The distribution ratio of Cu between the flux and molten iron, $L_{Cu(\text{flux-Fe})}$, is expressed as a product of $L_{Cu(\text{flux-Ag})}$ and $L_{Cu(\text{Ag-Fe})}$. The value of $L_{Cu(\text{Ag-Fe})}$ measured in our previous work is 7.15[9] in the region of the dilute solution. In this work, the largest value of $L_{Cu(\text{flux-Ag})}$ is 17 at a partial oxygen pressure of 0.6 atm. Accordingly, $L_{Cu(\text{flux-Fe})}$ is estimated to be up to approximately 120.

On the other hand, the oxidation of Ag is expressed as follows[11].

$$2Ag(l)+1/2O_2(g)=Ag_2O(s) \tag{8}$$

$$\Delta G^{\circ}_{(8)} = -53100+84.1T\ (\text{J/mol}) \tag{9}$$

Because pure Ag_2O is decomposed entirely at 1523 K, the standard of activity is selected as solid Ag_2O as was used by Wakasugi *et al*[15]. a_{Ag_2O} can be determined by the p_{O_2} because a_{Ag} is assumed to be nearly unity. Fig. 10 shows $\gamma_{Ag_2O(\text{in flux})}$ as a function of $N_{B_2O_3(\text{in flux})}$. The value of $\gamma_{Ag_2O(\text{in flux})}$ decreases with an increase in $N_{B_2O_3(\text{in flux})}$ and is smaller than that of $\gamma_{Cu_2O(\text{in flux})}$. The value of $\gamma_{Cu_2O(\text{in flux})}$ increases with an increase in p_{O_2} because the B_2O_3 content of the flux decreases as a result of the increase in $Ag(Ag_2O)$ content at high p_{O_2}, as shown in Fig. 7. As a result, there is an optimal p_{O_2} (0.6 atm) which maximizes the value of $L_{Cu(\text{flux-Ag})}$ as shown in Fig. 6.

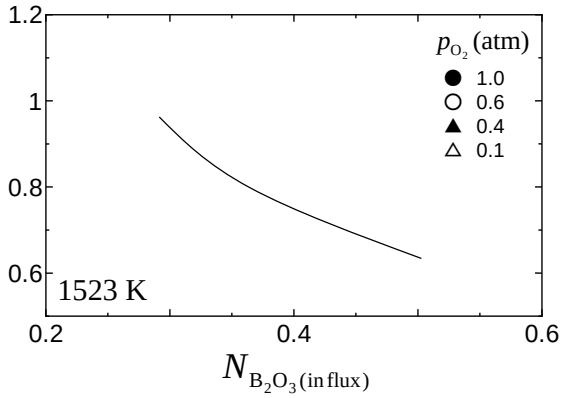

Fig. 9 Dependence of $\gamma_{Cu_2O(\text{in flux})}$ on $N_{B_2O_3(\text{in flux})}$ at 1523 K.

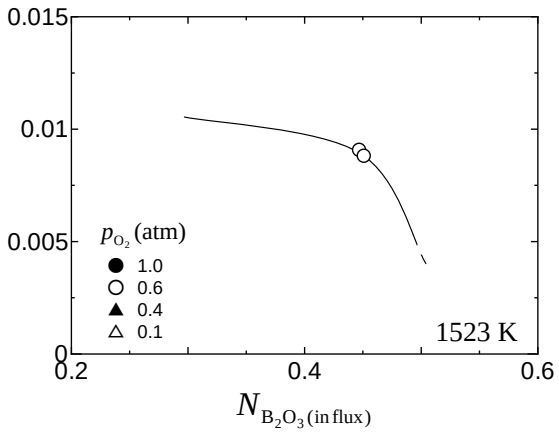

Fig. 10 Dependence of $\gamma_{Ag_2O(in\,flux)}$ on $N_{B_2O_3\,(in\,flux)}$ at 1523 K.

5.2 Behavior of solute elements in the oxidative removal of Cu from carbon-saturated iron via Ag phase into B_2O_3 flux

In Run 9, the Ag phase is separated at the path by $FeAl_2O_4$, which is formed by the reaction of Fe and O in the Ag phase with the alumina. In Run 10, the experiment, of which the apparatus is shown in Fig. 3 (b), is performed on condition that the path is widened sufficiently. As a result, molten iron is pushed from the inside to the exterior of the alumina tube. This is because the dissolved oxygen reaches the Fe-Ag interface, and the inner pressure of the alumina tube rises because of the CO gas generation. In Run 9, the molten iron is not pushed out of the tube because the transfer of oxygen inside the alumina tube is prevented. In a similar way, the distribution ratio of Cu between Fe-C(satd.) and Ag inside the alumina tube is equal to the equilibrium value (=7.15)[9] because transfer of the Cu is also prevented. Therefore, control of the oxygen supply is important.

On the other hand, the B_2O_3 flux is expected to control the amount of oxygen transported in Runs 12 and 13. However, oxidation of the Cu in the Ag phase does not occur because the dissolution rate of oxygen into the flux is low. On the other hand, the Cu is absorbed into the flux in the experiments using the B_2O_3-Al_2O_3-Ag_2O flux whose oxygen potential is high (Runs 14–17).

The cross sectional area at the path of Runs 16 and 17 is larger than that of Runs 14 and 15. As a result, the Cu and Ag are dissolved into the flux in Runs 14 and 15, and the Fe in addition to the Cu and Ag is dissolved into the flux in Runs 16 and 17. It is important to investigate the behavior of the Fe, Cu and O in the Ag in order to know the mechanism of the oxidative removal of Cu from carbon-saturated iron via Ag into B_2O_3 flux. Accordingly, a numerical calculation of mass transfer on the solutes in the Ag phase is tried in the next section.

5.3 Numerical calculation of mass transfer on the solutes in the Ag phase

The diffusion coefficients of Cu, Fe and O in the Ag at 1523 K are known to be 4.49×10^{-9} (m^2/s), 4.93×10^{-9} (m^2/s) and 1.76×10^{-8} (m^2/s), respectively[16]. The solubility of the oxygen in the Ag is 0.24 mass% at a partial oxygen pressure of 1 atm[17].

The one dimensional Ag phase whose length is 20 mm is defined for the calculation. The Fe-Ag interface and the Ag-flux interface are located at 0 and 20 mm, respectively. Initially, the behavior of the diffusion of Cu, Fe and O is calculated based on Fick's second law without consideration of the oxidative reaction. The calculation conditions are as follows:

(1) At 0 mm, the mole fractions of Cu and Fe in the Ag are fixed at 0.05 and 0.0012 (3.0 mass% and 0.06 mass%), respectively.

(2) At 0 mm, the mole fraction of O is fixed to be zero because the oxygen that reaches the Fe-Ag interface reacts with carbon in the Fe-C(satd.) and forms CO gas.

(3) At 20 mm, the mole fraction of Cu is fixed to be 0.0252 (1.5 mass%). This value is determined from our previous work performed without oxide flux at a partial oxygen pressure of 1 atm[9]. The mole fraction of the Fe is fixed to be zero because the transported Fe is fully oxidized.

(4) At 20 mm, the mole fraction of O is fixed to be 0.016 (0.24 mass%), which is the solubility of the oxygen in the Ag at a partial oxygen pressure of 1 atm.

The mole fractions of Cu, Fe and O are calculated based on these conditions, and their steady states are shown in Fig. 11. The contents are expressed as mole fraction, N_i (i = Cu, Fe, O). The absolute quantity of Cu is much larger than that of Fe.

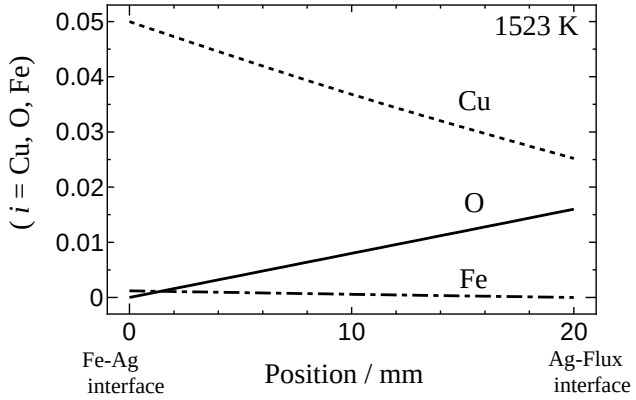

Fig. 11 The diffusion profiles of Cu, O and Fe in the Ag at the steady state when the oxidative reaction is not taken into account.

Therefore, the calculation is performed in consideration of the oxidative reaction of Cu and out of consideration of that of Fe. The calculation conditions are as follows:

(1) Under the initial condition, the mole fraction of Cu over the whole position is 0.05.

(2) The mole fraction of Cu at 0 mm is fixed at 0.05.

(3) Under the initial conditions, the mole fractions of O at 20 mm and the other position are 0.016 and 0, respectively.

(4) The Cu and O react immediately, and the formed Cu_2O is removed from the system.

(5) The lowering limit of Cu is 0.0252, which is the equilibrium value at a partial oxygen pressure of 1 atm.

The calculation result of the Cu and O mole fractions is shown in Fig. 12. The Cu content of the Ag decreases with time and reaches steady state in approximately 11 ks. The oxidative reaction occurs at a fixed position (4 mm), on condition that a stable supply of Cu and oxygen gas is provided and the length of the Ag phase is 20 mm. In a similar way, the O content increases with time, and the reaction achieves steady state for 11 ks. These results show that to keep the position of the oxidative reaction outside the alumina tube makes it possible to enhance the oxidative reaction of Cu and prevents the oxygen from being reached at the Fe-Ag interface. The steady states are shown in Fig. 13 where the initial mole fractions of Cu at the Fe-Ag interface are fixed to be 0.1, 0.05 and 0.04. As the initial mole fraction of Cu in the Fe-Ag interface decreases, the position of the oxidative reaction gradually moves to the negative direction. When the Cu content of the Fe-C(satd.) decreases, the Cu content of the Fe-Ag interface also decreases and the oxygen gets close to the Fe-Ag interface. When the Cu contents of the Fe-C(satd.) and Ag phases decrease and close to the equilibrium, the driving force of the Cu transfer is lost. As the result, oxygen in the Ag reaches the Fe-Ag interface and reacts with C in the Fe-C(satd.), and CO gas appears to be formed. In fact, oxygen reaches the Fe-Ag interface, and CO gas forms before the Cu content reaches the equilibrium in Runs 15-17. Because of the CO gas formation, a part of the Ag inside the alumina tube appears to be pushed out of the alumina tube in Run 15, and a part of the Fe and most of the Ag inside the alumina tube are pushed out in Runs 16 and 17. Besides, once the oxygen reaches inside the alumina tube, the formed Fe and Cu oxides appear to rise to the Fe-Ag interface and react with C in the Fe-C(satd.), which is also conductive to CO gas formation.

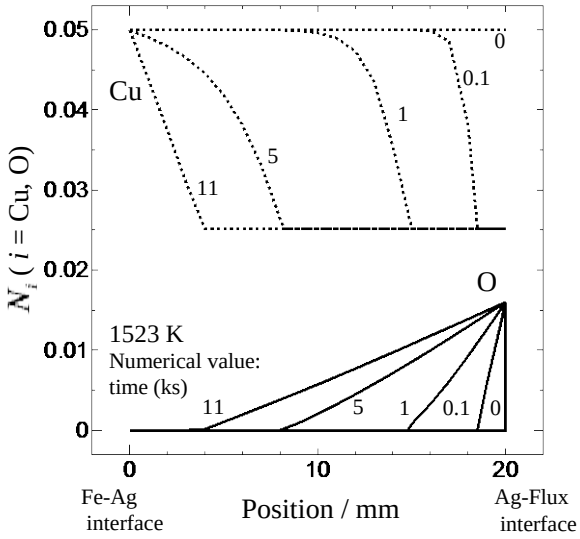

Fig. 12 Variation of the diffusion profiles of Cu and O in the Ag with time when the oxidative reaction is taken into account at 1523 K (Initial mole fraction of Cu in the Ag phase is 0.05).

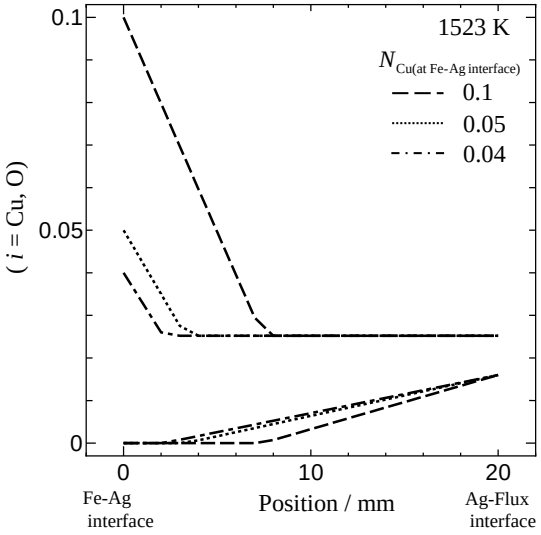

Fig. 13 Variation of the diffusion profiles of Cu and O in the Ag with the initial mole fraction of Cu at the Fe-Ag interface when the oxidative reaction is taken into account after 15 ks at 1523 K.

Under the experimental conditions of this work, oxygen will easily reach the inside of the alumina tube because the initial Cu content of the Fe-C(satd.) before oxidative removal is close to the equilibrium lower limit (0.26 mass%) at the conditions of $p_{O_2}(=1\text{atm})$ and $a_{Cu_2O}(=1)$, and the driving force of Cu transfer is low at the initial condition in this work. On the other hand, based on this discussion, the driving force is increased by decreasing a_{Cu_2O} with the oxide flux in this work. The result is shown in Fig. 14 when the lower limit of Cu in the Ag decreases to 0.01 (0.6 mass%) using the oxide flux. The value of a_{Cu_2O} is calculated to be 0.10 under this condition. Other calculating conditions are the same as the calculation in Fig. 12. As the result, the time to achieve steady state is 17 ks and the reaction position is 5 mm. By comparison of Fig. 14 with Fig. 12, the reaction position moves towards the Ag-flux interface by 1 mm and the time to reach steady state becomes long because the amount of reactive Cu increases. Accordingly, it is effective to use the oxide flux in order to ensure the driving force of Cu transfer and enhance Cu removal in this work.

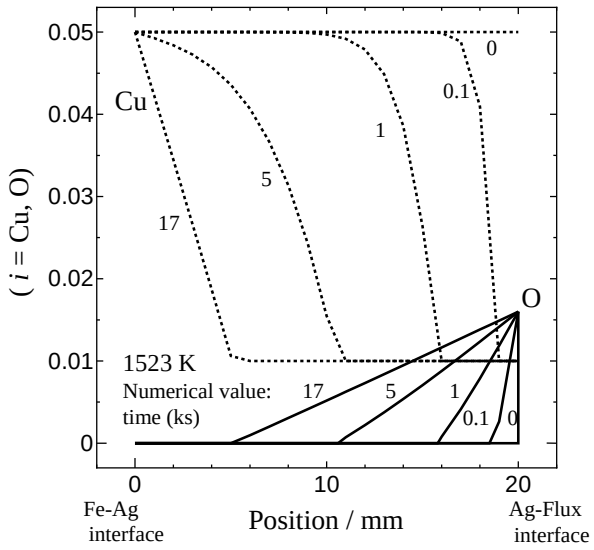

Fig. 14 Variation of the diffusion profiles of Cu and O in the Ag with time when the oxidative reaction is taken into account and the lowering limit of Cu is decreased by using flux at 1523 K.

6. Conclusion

In order to remove Cu in molten iron, the oxidative removal of Cu from the Fe-C(satd.) via Ag into the B_2O_3 flux is proposed and tried at 1523K. As the basis, the activity coefficient of Cu_2O in the B_2O_3 flux is measured at 1523K. The conclusions are as follows:

(1) B_2O_3 is one of the suitable flux for absorbing Cu because the $\gamma_{Cu_2O(\text{in flux})}$ value is smaller than unity. Not only Cu but also Ag is absorbed in the flux as an oxide. For this reason, there is a suitable oxygen partial pressure for the Cu removal. In this work, the largest value of the distribution ratio, $L_{Cu(\text{flux-Ag})}$ (= [mass% Cu]$_{(\text{in flux})}$ / [mass% Cu]$_{(\text{in Ag})}$), is 17 at an oxygen partial pressure of 0.6 atm. The value of $L_{Cu(\text{flux-Fe})}$ (= [mass% Cu]$_{(\text{in flux})}$ / [mass% Cu]$_{(\text{in Fe-C})}$) is estimated to be approximately 120 from the product of $L_{Cu(\text{flux-Ag})}$ and $L_{Cu(\text{Fe-Ag})}$.

(2) The Cu in Fe-C(satd.) can remove effectively by applying the oxidative removal via Ag into the B_2O_3(-Al_2O_3-Ag_2O) flux proposed in this work.

(3) From a numerical calculation, it is found to be effective to use the oxide flux in order to decrease the lower limit of Cu, to ensure the driving force of Cu transfer and to enhance the continuous Cu removal.

Acknowledgment

We would like to thank the Iron and Steel Institute of Japan for the financial support of "ISIJ Research Promotion Grant".

References

[1] The Japan Ferrous Raw Materials Association. Annual report of iron source, The Japan Ferrous Raw Materials Association, Tokyo, 2011, p30, in Japanese.

[2] M. Iwase and K. Tokinori. A Feasibiligy Study for the Removal of Copper from Solid Ferrous Scrap. *Steel*

Research, 1991, 62(6), p235-239.

[3] M. Iwase, K. Tokinori and H. Ohshita. Separation of Copper from Solid Ferrous Scrap by Using Molten Aluminum. *Iron Steelmaker*, 1993, 20(7), p61-66.

[4] M. Iwase and H. Ohshita. Further Studies of the Removal of Copper from Solid Scrap. *Steel Research*, 1994, 65(9), p362-367.

[5] K. Zhou, K. Shinme and S. Anezaki. Dissolution Rate of Copper in Aqueous Ammonia Solution. *Journal of MMIJ*, 1995, 111(1), p49-53, in Japanese.

[6] K. Yamaguchi and Y. Takeda. Copper Enrichment of Scrap by Phase Separation in Liquid Fe-Cu-C System. *Shigen-to-Sozai*, 1997, 113(12), p1110-1114, in Japanese.

[7] K. Marukawa, T. Tanaka and S. Hara. Recycle of Iron-Copper Mixed Scrap by Using Liquid Immiscibility. *Eng. Mater.*, 2000, 48(3), p62-65, in Japanese.

[8] K. Taguchi, H. Ono-Nakazato, T. Usui. Liquid Immiscibility in Fe-Cu-B System. *ISIJ Int.*, 2006, 46(1), p29-32.

[9] K. Yamaguchi, H. Ono and T. Usui. Oxidation Removal of Cu from Carbon Saturated Iron via Ag Phase. *Tetsu-to-Hagané*, 2010, 96(9), p531-535, in Japanese.

[10] H. Ono, Y. Tanaka, K. Yamaguchi and T. Usui. Oxidation Removal of Sn from Carbon Saturated Iron via Ag Phase. *Tetsu-to-Hagané*, 2010, 96(11), p641-645, in Japanese.

[11] E.T. Turkdogan. Physical Chemistry of High Temperature Technology, Academic Press, New York, 1980, p5, 10.

[12] K. Morinaga, H. Yoshida and H. Takebe. Compositional Dependence of Absorption Spectra of Ti^{3+} in Silicate, Borate, and Phosphate Glasses. *J. Am. Ceram. Soc.*, 1994, 77(12), p3113-3118.

[13] P.J.M. Gielisse and W.R. Foster. The System Al_2O_3-B_2O_3. *Nature*, 1962, 195, p69-70.

[14] R. Hultgren, P. Desai, D. Hawkins, M. Gleiser and K.K. Kelley. Selected Values of the Thermodynamic Properties of Binary Alloys, American Society for Metals, Metal Park, Ohio, 1968, p44.

[15] T. Wakasugi, A. Hirota, J. Fukunaga and R. Ota. Solubility of Ag_2O into the Na_2O–B_2O_3–Al_2O_3 system. *J. Non-Cryst. Solids*, 1997, 210(2-3), p141-147.

[16] The 140th Committee of Japan Society for Promotion of Science. Handbook of Physico-chemical Properties at High Temperatures, ed. by Y. Kawai and Y. Shiraishi, ISIJ, Tokyo, 1988, p184, 185.

[17] I.D. Shah and N.A.D. Parlee. The Diffusivity of Oxygen in Liquid Silver. *Trans. Metall. Soc. AIME*, 1967, 239(5), p763-764.